Unsteady flow of an electrically conducting dusty-gas in a channel due to an oscillating pressure gradient

Ali J. Chamkha

Kuwait University, Department of Mechanical Engineering, Safat, Kuwait

Equations governing transient, laminar, hydromagnetic flow of a two-phase particulate suspension having a finite particulate volume fraction in a channel are developed. These equations are solved analytically in terms of cosine Fourier series subject to appropriate conditions by the separation of variables method. The flow of the suspension in the channel is assumed to take place due to the application of a time-dependent oscillating pressure gradient. The influence of the Hartmann number, particle loading, and the inverse Stokes number on the fluid and particle volume flow rates and the fluid-phase skin-friction coefficient is illustrated graphically. Comparisons with previously published work are made, and interpretation of the solutions is discussed.

Keywords: Two-phase flow, unsteady flow, MHD channel flow, oscillating pressure gradient

1. Introduction

The problem considered in this paper is that of the transient flow of nonconducting particles suspended in an electrically conducting fluid in a channel in the presence of a transverse magnetic field due to an oscillating pressure gradient applied parallel to the channel walls. The flow is assumed to be laminar and incompressible, and the particle-phase is assumed to have a constant finite volume fraction. This problem is chosen due to its occurrence in many industrial engineering applications and because the governing equations can be solved in closed form. This is important because these closed-form solutions can serve as known solutions for parameter effects and the calibration of numerical solutions and can be used as tools for design and understanding of flow behavior in systems involving such situations. In general, there are two basic approaches to modelling two-phase fluid-particle flows. These are based on the Eulerian and the Lagrangian descriptions known from fluid mechanics. The former treats both the fluid and the particle phases as interacting continua (see Marble,[1] Soo[2], and Ishii [3]), while the latter treats only the fluid phase as a continuum with the particle phase being governed by the kinetic theory (see Berloment et al.[4]). The present work employs the continuum approach and employs the dusty-gas equations (meant for the description of particulate suspensions having a small volume fraction) discussed by Marble[1], modified for finite particle volume fraction and including a hydromagnetic body force.

Previously published related work can be found in the papers by Ritter and Peddieson,[5] Chamkha,[6-8] Mitra and Bhattacharyya,[9] Tseng and Sahai,[10] and the book by White.[11] It is sought herein to develop closed-form solutions for the velocity profiles, skin-friction coefficient, and the volume flow rates for both phases, which extend the solutions presented by Ritter[12] to electrically conducting fluid-particle suspensions. The fluid phase will be assumed incompressible, and the particle phase will be assumed to be pressureless. The particles will be assumed to be dragged along by the fluid motion. The drag force between the phases is based on Stokes' linear drag theory. In addition the induced magnetic field and the Hall effect of magnetohydrodynamics are neglected in the present work.

2. Governing equations

Consider transient one-dimensional plane flow of a particulate suspension through a horizontal channel due to the application of a time-dependent oscillating pressure gradient applied in the horizontal direction. A uniform magnetic field is applied normally to the flow direction (see *Figure 1*). The channel is assumed to have infinite length, such that the dependence of the flow variables on the horizontal direction is negligible. The suspended particles are all of one size and are uniformly distributed.

Address reprint request to Dr. Chamkha at Kuwait University, Department of Mechanical Engineering, 13060 Safat, Kuwait.

Received 11 October 1995; revised 6 January 1997; accepted 17 February 1997.

Appl. Math. Modelling 1997, 21:287–292, May

655 Avenue of the Americas, New York, NY 10010

0307-904X/97/$17.00
PII S0307-904X(97)00018-8

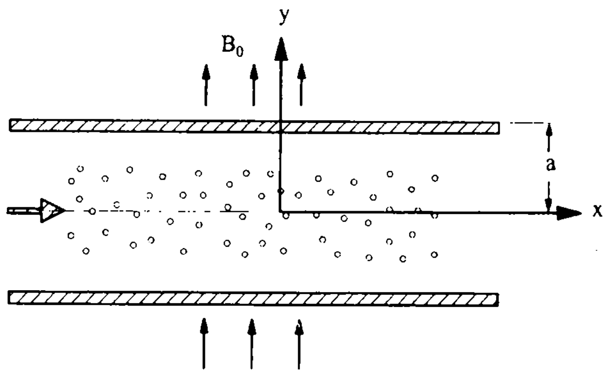

Figure 1. Problem definition.

The governing equations for this investigation are based on the balance laws of mass and linear momentum of both phases. As mentioned before the continuum formulation of these laws is employed in the present work (see, for instance, Soo[2]). These are given by

$$\partial_t\phi - \vec{\nabla}\cdot\left((1-\phi)\vec{V}\right) = 0,$$
$$\partial_t\phi + \vec{\nabla}\cdot\left(\phi\vec{V}_p\right) = 0$$
$$\rho(1-\phi)\left(\partial_t\vec{V} + \vec{V}\cdot\vec{\nabla}\vec{V}\right) = \vec{\nabla}\underline{\underline{\sigma}} - \vec{f} + \vec{b}$$
$$\rho_p\phi\left(\partial_t\vec{V}_p + \vec{V}_p\cdot\vec{\nabla}\vec{V}_p\right) = \vec{\nabla}\cdot\underline{\underline{\sigma}}_p + \vec{f} + \vec{b}_p \qquad (1)$$

where t is time, ϕ is the particle-phase volume fraction, $\vec{\nabla}$ is the gradient operator, $\vec{V}$ is the fluid-phase velocity vector, $\vec{V}_p$ is the particle-phase velocity vector, ρ is the fluid-phase density, ρ_p is the particle-phase in-suspension density, $\underline{\underline{\sigma}}$ is the fluid-phase stress tensor, $\underline{\underline{\sigma}}_p$ is the particle-phase stress tensor, $\vec{f}$ is the interphase force per unit volume acting on the particle phase, $\vec{b}$ is the fluid-phase body force per unit volume, and $\vec{b}_p$ is the particle-phase body force per unit volume.

To completely define the problem, additional constitutive equations for the fluid- and particle-phase stress tensors, the interphase force, and the body forces are needed. These are assumed, respectively, as

$$\underline{\underline{\sigma}} = (1-\phi)\Big((-P + \lambda^*\vec{\nabla}\cdot\vec{V})\underline{\underline{I}} + \mu(\phi)\left(+\vec{\nabla}\vec{V} + \vec{\nabla}\vec{V}^T\right)\Big)$$
$$\underline{\underline{\sigma}}_p = 0, \vec{f} = N(\phi)\rho_p\phi\left(\vec{V} - \vec{V}_p\right)$$
$$\vec{b} = \rho\vec{g} + \sigma_1(\vec{V}\times\vec{B})\times\vec{B}, \vec{b}_p = \rho_p\vec{g} \qquad (2)$$

where P is the fluid pressure, $\underline{\underline{I}}$ is the unit tensor, μ, is the fluid dynamic viscosity, λ^* is the bulk coefficient of viscosity, σ_1 is the fluid electrical conductivity, $\vec{B}$ is the magnetic induction field, N is the momentum transfer coefficient, $\vec{g}$ is the gravitational acceleration vector, and a superscript T indicates the transpose of a second-order tensor. In the present work the particle phase is assumed to be stress free, such that the suspension is dilute and no particle-particle interaction exists (see Marble [1]). In addition, ϕ, ρ, ρ_p, μ, and N are all assumed constant.

In reality the volume fraction of particles in the suspension is not constant. The assumption of constant and uniform distribution of ϕ is an idealization and is applicable in limited situations. This is done herein so as to allow the governing equations to be solved in closed form. There have been some published works that predict variable particle volume fraction (see, for instance, Soo,[13] Sinclair and Jackson,[14] and Drew and Lahey[15]). The inclusion of a lift force in the equations is sufficient (but not necessary) to produce nonuniform volume fraction distribution. It should be noted that in the present work the hydrodynamic interactions between the phases are limited to the drag force. This assumption is feasible when the particle Reynolds number is assumed to be small. Other interactions such as the virtual mass force (Zuber[16]), the shear force (Saffman[17]), and the spin-lift force (Rubinow and Keller[18]) are assumed to be negligible compared to the drag force (see, for instance, Apazidis[19]).

It is convenient to work with nondimensional equations. The following equations are used to accomplish this task.

$$y = a\eta, t = (a^2\tau)/\nu, \frac{\partial p}{\partial x} = -G_0G(\tau)$$
$$\vec{V} = (G_0a^2)/\mu F(\eta,\tau)\vec{e}_x$$
$$\vec{V}_p = (G_0a^2)/\mu F_p(\eta,\tau)\vec{e}_x$$
$$\rho_p = \kappa\rho D_p(\eta), D_p(y,0) = 1$$
$$\kappa = \rho_p\phi/(\rho(1-\phi)), \vec{g} = -g\vec{e}_y, \vec{B} = B_0\vec{e}_y \qquad (3)$$

(where $\vec{e}_x$ and $\vec{e}_y$ are unit vectors in the x- and y-directions, respectively, "a" is the channel half width, $\nu = \mu/\rho$, and G_0 and B_0 are constants). It should be noted that while it is obvious that the density difference between the constituents of the suspension will initiate a separational motion of the phases in the vertical direction it is assumed that the velocity fields of both phases are parallel to the boundaries of the channel. This is because the channel is assumed to be infinitely long, a necessary assumption to allow for a closed-form solution.

Substituting equations (2) (with $\lambda^* = 0$) and (3) into equations (1), simplifying, and then rearranging yield the following dimensionless equations

$$\frac{\partial F}{\partial \tau} = \frac{\partial^2 F}{\partial \eta^2} + \kappa\alpha D_p(F_p - F) - M^2F + G(\tau) \qquad (4)$$

$$\frac{\partial F_p}{\partial \tau} = \alpha(F - F_p) \qquad (5)$$

where $\alpha = (Na^2)/\nu$ and $M = (\sigma_1/\mu)^{1/2}B_0a$ are the inverse Stokes number and the Hartmann number, respectively. Equations (3) and (4) will be solved subject to the following initial and boundary conditions

$$F(\eta,0)=0, F_p(\eta,0)=0, F(1,\tau)=0$$

$$F_p(1,\tau)=0, \frac{\partial F}{\partial \eta}(0,\tau)=0, \frac{\partial F_p}{\partial \eta}(0,\tau)=0 \qquad \text{(6a–f)}$$

Equations (6a) and (6b) indicate that the fluid and the particles are initially at rest. Equations (6c) and (6d) suggest that both the fluid and the particle phases do not slip at the surfaces. Equations (6e) and (6f) are symmetry conditions for the fluid and particle phases, respectively.

3. Results and discussion

Solutions will be obtained for uniform particle-phase density ($D_p = 1$) by using Fourier cosine series of the form

$$F(\eta,\tau)=\sum_{n=1}^{\infty} F_n(\tau)\cos(\lambda_n \eta)$$

$$F_p(\eta,\tau)=\sum_{n=1}^{\infty} F_{pn}(\tau)\cos(\lambda_n \eta) \qquad (7)$$

where $\lambda_n = (2n-1)\pi/2$ and $F_n(\tau)$ and $F_{pn}(\tau)$ are to be determined.

Substituting equations (7) into equations (5) and (6), multiplying each equation $\cos(\lambda_m \eta)$ and then integrating each equation with respect to η from $\eta = 0$ to $\eta = 1$ gives

$$\dot{F}_n + \lambda_n^2 F_n - \kappa\alpha(F_{pn} - F_n) - M^2 F_n - \frac{2(-1)^{n+1}}{\lambda_n} G(\tau) = 0 \qquad (8)$$

$$\dot{F}_{pn} - \alpha(F_n - F_{pn}) = 0 \qquad (9)$$

where a dot represents ordinary differentiation with respect to τ.

Solving for F_{pn} from equation (8), taking the necessary derivatives, and then substituting into equation (9) leads to a second-order equation in F_n. This can be written as

$$\ddot{F}_n + (M^2 + \lambda_n^2 + \alpha(1+\kappa))\dot{F}_n + \alpha(M^2 + \lambda_n^2)F_n = a_n(\dot{G}(\tau) + G(\tau)) \qquad (10)$$

where

$$a_n = 2(-1)^{n+1}/\lambda_n \qquad (11)$$

Let the applied pressure gradient $G(\tau)$ be a sinusoidal function of time as follows

$$G(\tau) = G_s \sin(\omega\tau) + G_c \cos(\omega\tau) \qquad (12)$$

where G_s, G_c, and ω are constants.

Differentiating equation (12) with respect to τ and then substituting into equation (10) results in

$$\ddot{F}_n + (M^2 + \lambda_n^2 + \alpha(1+\kappa))\dot{F}_n + \alpha(M^2 + \lambda_n^2)F_n = a_n((G_s\alpha - G_c\omega)\sin(\omega\tau) + (G_c\alpha + G_s\omega)\cos(\omega\tau)) \qquad (13)$$

Both the fluid and particle phases start from rest. This is represented by the initial conditions

$$F_n(\eta,0)=0,\ F_{pn}(\eta,0)=0 \qquad (14)$$

The initial-value problem given by equations (13) and (14) can be solved exactly by the usual methods of solving such problems. The homogeneous part of the general solution of F_n can be shown to be

$$F_{nh} = C_1 \exp(m_1\tau) + C_2 \exp(m_2\tau) \qquad (15)$$

where

$$m_1 = \left(-B + (B_1^2 - 2A_1)^{1/2}\right)/2$$

$$m_2 = \left(-B_1 - (B_1^2 - 4A_1)^{1/2}\right)/2$$

$$B_1 = M^2 + \lambda_n^2 + \alpha(1+\kappa),\ A_1 = \alpha(M^2 + \lambda_n^2) \qquad (16)$$

and C_1 and C_2 are arbitrary constants to be determined.

It is important to check whether m_1 and m_2 can be complex or not. This depends on the sign of $\Delta = B_1^2 - 4A_1$. If $\Delta < 0$, then complex numbers result. However, if $\Delta \geqslant 0$, then m_1 and m_2 will not be complex numbers. It can be shown that

$$\Delta = B_1^2 - 4A_1 = (M^2 + \lambda_n^2)(M^2 + \lambda_n^2 + 2\alpha(\kappa - 1)) + \alpha^2(1+\kappa)^2 \qquad (17)$$

The typical physical range of values for α and κ are $0 \leqslant \alpha \leqslant 100$ and $0 \leqslant \kappa \leqslant 100$. For these ranges it can easily be shown that Δ will always be positive and, therefore, m_1 and m_2 will always be real.

The particular solution for F_n from equation (13) can be written as

$$F_{pn} = C_3 \sin(\omega\tau) + C_4 \cos(\omega\tau) \qquad (18)$$

where

$$C_3 = (X_1 Z_1 + Y_1 Z_2)/(X_1^2 + Y_1^2)$$

$$C_4 = (X_1 Z_2 + Y_1 Z_1)/(X_1^2 + Y_1^2)$$

$$X_1 = A_1 - \omega^2, Y_1 = B_1\omega$$

$$Z_1 = a_n(G_s\alpha - G_c\omega), Z_2 = a_n(G_s\alpha + G_c\omega) \qquad (19)$$

Thus the general solution for F_n can now be written as

$$F_n = C_1 \exp(m_1\tau) + C_2 \exp(m_2\tau) + C_3 \sin(\omega\tau) + C_4 \cos(\omega\tau) \qquad (20)$$

where

$$C_2 = (C_4 m_1 - C_3 \omega + a_n G_c)/(m_2 - m_1)$$
$$C_1 = -C_2 - C_4 \tag{21}$$

are found by the application of the initial conditions. With the solution of F_n known, the solution for F_{pn} can be shown to be

$$F_{pn} = \frac{1}{\kappa\alpha}(C_1(m_1 + (M^2 + \lambda_n^2 + \kappa\alpha))\exp(m_1\tau) + C_2(m_2 + (M^2 + \lambda_n^2 + \kappa\alpha))\exp(m_2\tau) + (C_3\omega + C_4(M^2 + \lambda_n^2 + \kappa\alpha) - a_n G_c)\cos(\omega\tau) + (-C_4\omega + C_3(M^2 + \lambda_n^2 + \kappa\alpha) - a_n G_s) \times \sin(\omega\tau)) \tag{22}$$

Of special interest is the fluid-phase volume flow rate, the particle-phase volume flow rate, and the fluid-phase skin-friction coefficient. These are given, respectively, by the following relations:

$$Q = 2\int_0^1 F(\eta,\tau)d\eta = 2\sum_{n=1}^{\infty} \frac{(-1)^{n+1}}{\lambda_n} F_n$$
$$Q_p = 2\int_0^1 F_p(\eta,\tau)d\eta = 2\sum_{n=1}^{\infty} \frac{(-1)^{n+1}}{\lambda_n} F_{pn}$$
$$C = -\frac{\partial F(1,\tau)}{\partial \eta} = \sum_{n=1}^{\infty} (-1)^{n+1}\lambda_n F_n \tag{23}$$

It should be noted that the total flow rates of the fluid and the particle phases are twice that of the calculated domain (as shown in equation [23]). This is due to the symmetry of the channel geometry.

A major objective of this work is to observe the variations of the fluid and particle volumetric flow rates and the fluid-phase skin-friction coefficient for various values of the inverse Stokes number α, the particle loading κ, and the Hartmann number M. For this purpose, numerical evaluations of equation (23) are made and the results are presented graphically in *Figures 2* through *10* to illustrate the flow behavior. It is seen from the solutions for F_n and F_{pn} presented earlier that they consist of two parts, an exponential part and an oscillatory part, which takes over when the exponential part approaches zero for large time values. The numerical calculations of these figures are carried out to about 3π time units to show the uniform oscillatory behavior of the quantities after the exponential part of the solutions decays.

Figures 2 through *4* illustrate the changes of Q, Q_p, and C with time for various values of κ, respectively. Physically speaking, as the particle concentration increases, the fluid phase experiences a larger drag force, which causes the carrier fluid (and consequently the particulate material) to slow down. This causes lower values in Q, Q_p, and C. As is evident from *Figures 5* and *6* the flow of the suspension in the channel becomes harder as κ becomes very large. In fact, there is very little flow of the fluid, and the particles for $\kappa = 100$ for the channel become clogged with particles.

Figures 5 through *7* present the respective transient variations of Q, Q_p, and C as α varies. Increases in the

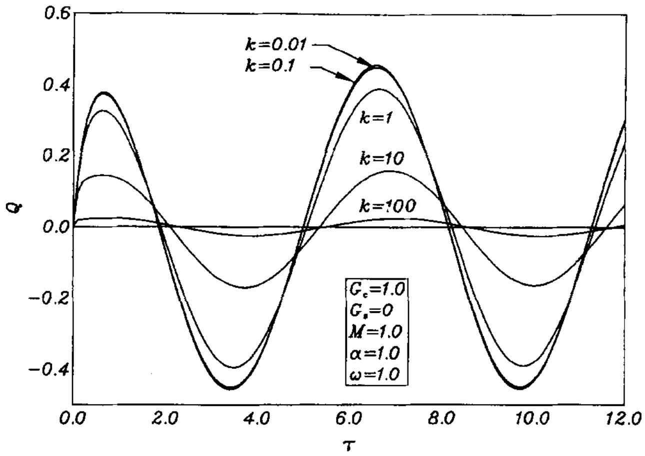

Figure 2. Fluid-phase volume flow rate time history.

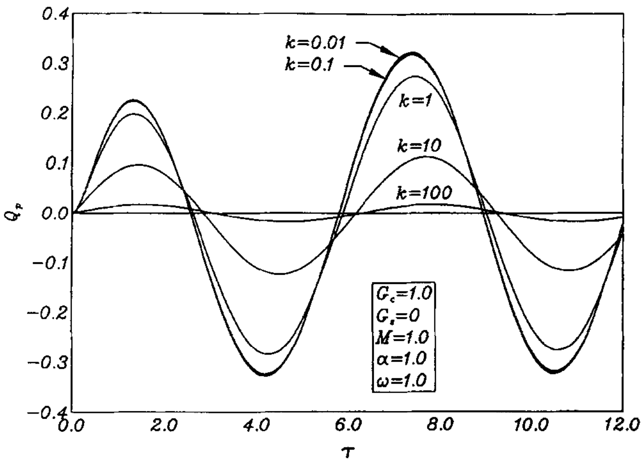

Figure 3. Particulate-phase volume flow rate time history.

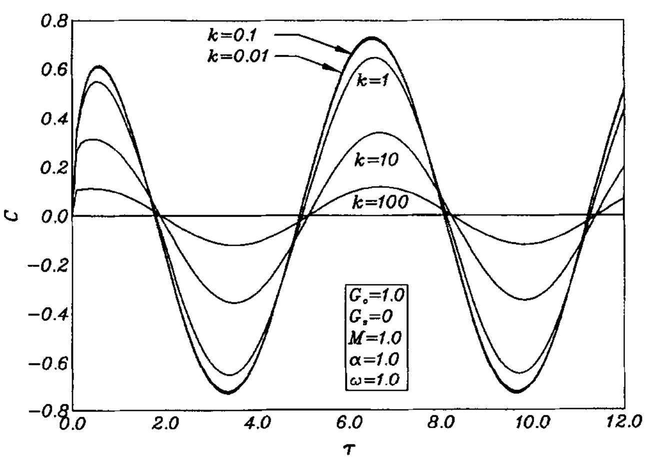

Figure 4. Fluid-phase skin-friction coefficient time history.

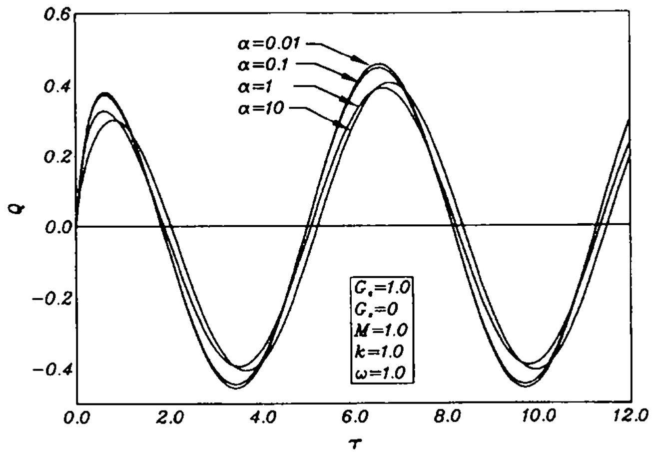

Figure 5. Fluid-phase volume flow rate time history.

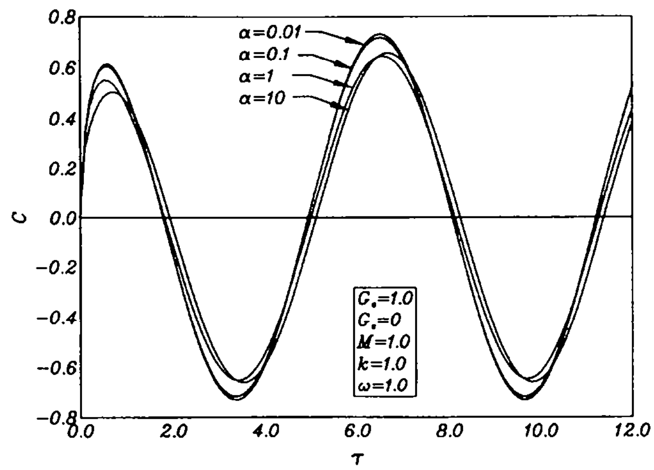

Figure 7. Fluid-phase skin-friction coefficient history.

values of α increase the hydrodynamic interaction (through the interphase drag force) between the phases. The presence of the particles in the flow tends to slow the fluid phase, and the particles will be dragged along with the carrier fluid which increases their velocities. This causes the volume flow rate of fluid-phase Q and correspondingly, the fluid-phase skin-friction coefficient C to decrease and the volume flow rate of the particle phase Q_p to increase. This behavior is evident from *Figures 2* through *4*.

Figures 8 through *10* show the transient behavior of Q, Q_p, and C as the Hartmann number M is varied. Increases in the values of M have the tendency to slow the movement of the suspension in the channel, causing a reduction in the flow rates of both phases and in the fluid wall shear stress. This is clearly depicted in the decreases of Q, Q_p, and C shown in *Figures 8* through *10* as M increases. It is observed in all the graphic results presented herein that the particle-phase motion in the channel lags behind that of the fluid phase. This is suggested from the occurrence of the peaks of Q earlier than those of Q_p. As mentioned before, for large values of τ the end conditions for the fluid- and particle-phase velocities in the channel will be uniform and oscillatory. These conditions occur after the exponential part of the solution decays. This means that the lag in the velocity of the particle phase with respect to the fluid phase and, therefore, the drag force will then remain constant.

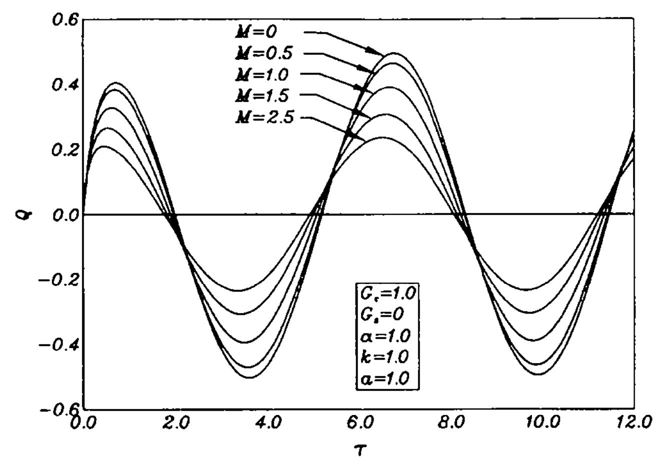

Figure 8. Fluid-phase volume flow rate time history.

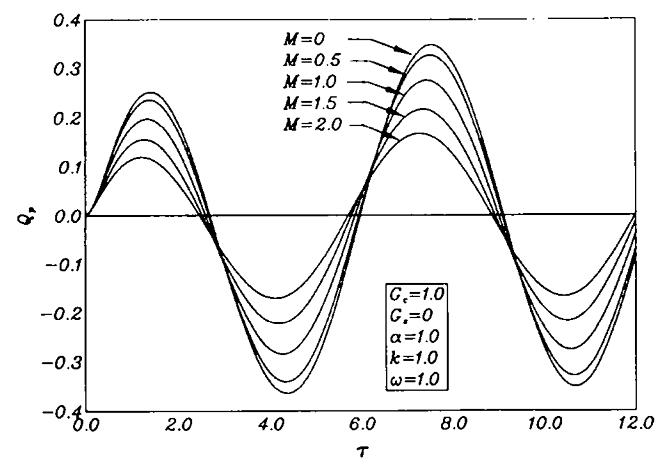

Figure 9. Particle-phase volume rate time history.

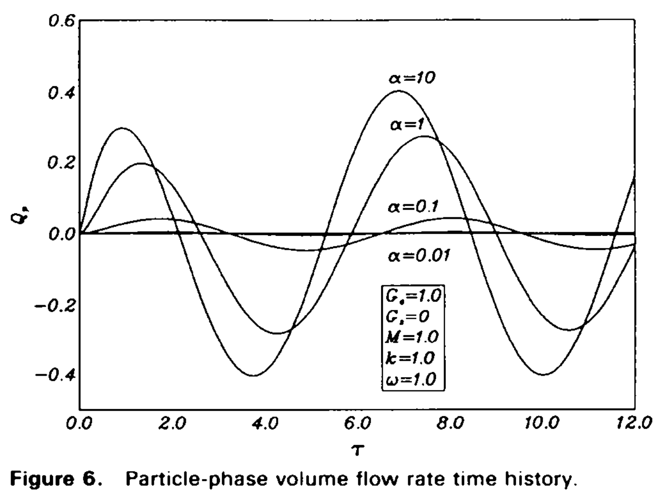

Figure 6. Particle-phase volume flow rate time history.

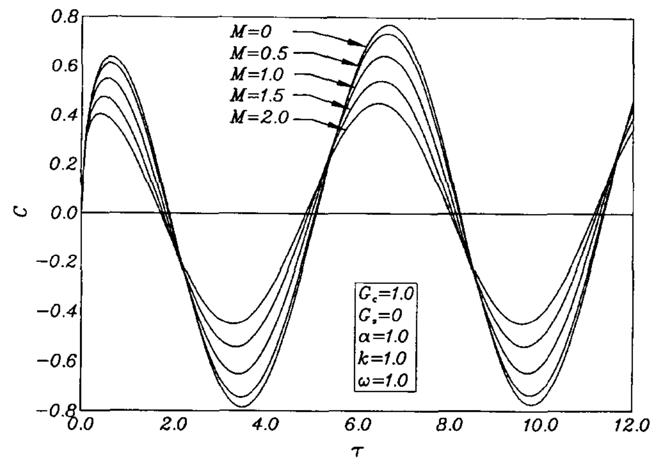

Figure 10. Fluid-phase skin-friction coefficient time history.

The exponential part of the close-form solutions given earlier has significance only in the initial stages of the flow. The uniform oscillatory behavior of the solutions is clearly observed from the results presented for small values of α and κ ($\alpha = 0.01$, $\kappa = 0.01$) are around 2π time units. However, as expected, in all other cases for larger values of α and κ this condition occurs at a shorter time since increases in these values introduce more damping effects into the motion of the suspension. It is seen from *Figures 2* through *10* that variations in the values of κ and M impact the results more significantly than that caused by variations in the values of α.

For the parametric values chosen for $G(\tau)$ in producing the graphic results, $G(\tau)$ is always less than or equal to unity. Thus the maximum values of Q, Q_p, C, and C_p are less than the steady-state values obtained for a constant pressure gradient ($G(\tau) = 1$) discussed by Chamkha.[6] When M is set to zero in the closed-form solutions presented herein, Ritter's[12] solutions are recovered. This lends confidence in the correctness of the exact solutions.

4. Conclusions

Continuum equations governing laminar flow of a two-phase particulate suspension in a channel due to an oscillating pressure gradient in the presence of a transverse magnetic field were developed. With the assumptions of incompressibility and constant particulate volume fraction the resulting equations were solved analytically in terms of cosine Fourier series using the separation-of-variable method. Numerical evaluations of the series solutions were performed (via a FORTRAN program) and were shown graphically to illustrate the effects of different physical parameters on the solutions. It was found that decreases in the fluid-phase volume flow rate, the particle-phase volume flow rate, and the fluid-phase skin-friction coefficient were produced by increases in the particle loading in the channel. This same behavior was observed as the strength of the applied magnetic field was increased. Comparisons with previously published results for special cases of this work were made, and the results were found to be in excellent agreement. It is hoped that the present analytical results will be of use in validating computer routines for numerical solutions of more complex two-phase particulate suspension flows in channels and in stimulating needed experimental work in this area.

References

1. Marble, F. E. Dynamics of dusty gases. *Annu. Rev. Fluid Mech.* 1970, **2**, 397
2. Soo, S. L. *Multiphase Fluid Dynamics*. Science Press, New York, 1990
3. Ishii, M. *Thermo-Fluid Dynamic Theory of Two-Phase Flow*. Eyrolles, Paris, 1975
4. Berlemont, A. et al. Particle Lagrangian simulation in turbulent flows. *Int. J. Multiphase Flow* 1990, **16**, 19
5. Ritter, J. M., and Peddieson, J. Transient two-phases flows in channels and circular pipes. *Proceeding of the Sixth Canadian Congress of Applied Mechanics* 1977
6. Chamkha, A. J. Series solution for closed-form unsteady hydromagnetic two-phase Poiseuille flow. Engineering Science Preprint 28.91029, 1991
7. Chamkha, A. J. Hydromagnetic two-phase flow in a channel. *Int. J. Eng. Sci.* 1995, 33, 437
8. Chamkha, A. J. Closed-form solutions for unsteady two-phase flow in a channel. *Advance in Filtration and Separation Technology* 1995, 9, 349
9. Mitra, P., and Bhattacharyya, P. On the hydromagnetic flow of a dusty fluid between two-parallel plates, one being stationary and the other oscillating. *J. Phys. Soc. Jpn.* 1981, **50**, 995
10. Tseng, A. A., and Sahai, V. Magnetohydrodynamic flow of a suspension in pipes. *Dev. Theoret. Appl. Mech.* 1982 **11**, 397
11. White, F. *Viscous Fluid Flow*. McGraw-Hill, New York, 1974
12. Ritter, J. M. Two-phase fluid flow in pipes and channels. M. S. Thesis, Tennessee Technological University, 1976
13. Soo, S. L. Pipe flow of suspensions. *Appl. Sci. Res.* 1969, **21**, 68.
14. Sinclair, J. L., and Jackson, R. Gas-particle flow in a vertical pipe with particle-particle interactions. *AIChE J.* 1989, **35**, 1473
15. Drew, D., and Lahey, R. T. Phase distribution mechanisms in turbulent two-phase flow in a circular pipe, *J. Fluid Mech.* 1982, **117**, 91
16. Zuber, N. On the dispersed two-phase flow in a laminar flow region. *Chem. Eng. Sci* 1964, **19**, 897
17. Saffman, P. G. The lift-force on a small sphere in a slow shear flow. *J. Fluid Mech.* 1965, **22**, 385
18. Rubinow, S. I. and Keller, J. B. The transverse force on a spinning sphere moving in a viscous fluid. *J. Fluid Mech.* 1961, **11**, 447
19. Apazidis, N. On two-dimensional laminar flows of a particulate suspension in the presence of gravity field. *Int. J. Multiphase Flow* 1985, **11**, 675